THE JOURNAL OF PHYSICAL CHEMISTRY LETTERS
A JOURNAL OF THE AMERICAN CHEMICAL SOCIETY

pubs.acs.org/JPCL

Letter

Bond-Breaking Reactions Encounter Distinct Solvent Environments Causing Breakdown of Linear Response

Andy Vong and Benjamin J. Schwartz*

Cite This: *J. Phys. Chem. Lett.* 2022, 13, 6783−6791

Read Online

ACCESS | Metrics & More | Article Recommendations | Supporting Information

ABSTRACT: Solvent effects are important for understanding solution-phase chemical reactions. Surprisingly, very few studies have explored how solvent dynamics change during the course of a reaction with solutes that encounter a wide range of configurations. Here, we use quantum simulation methods to explore the solvent dynamics during a solution-phase bond-breaking reaction: the photodissociation of Na_2^+ in liquid Ar. We find that the solute experiences a small number of distinct solvent environments that change in a discrete fashion as the bond lengthens. In characterizing the solvent environments, we show also that linear response fails by all measures, even when nonstationarity of solvent dynamics is considered. This observation of distinct solvent response environments with a solvent that can undergo only translational motions highlights the complexity of solute−solvent interactions, but that there are only a few environments gives hope to the idea that solvation dynamics can be understood for solution-phase reactions that explore a wide configuration space.

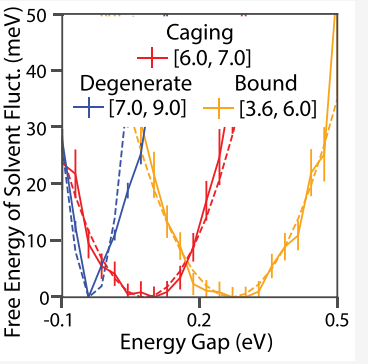

Solvents can affect chemical dynamics in a variety of ways that are important for understanding solution-phase chemistry. For example, solvents can allow reactants to encounter each other by diffusion and can stabilize or destabilize reactant transition states.[1,2] Solvent motions also drive electron and proton transfer reactions,[3−5] and the local solvation environment can break the symmetry of symmetric molecules as well as induce dipole moments.[6−9] Perhaps even more surprisingly, when there are modest local specific interactions between solvents and solutes, the solvent can become part of the chemical identity of a solution-phase reacting species.[10,11]

The way that solvents affect chemical reactivity can change dynamically during the course of a reaction, adding an additional layer of complexity. Under the linear response (LR) approximation, the solvent dynamics at the start of a reaction should match those associated with the initial solute state (the ground state in a photochemical reaction). At longer times, when a reaction is near completion, however, one expects that the solvent dynamics will match those associated with the equilibrium final state (the excited state in a photochemical reaction).[12−14] For a number of chemical reactions, and particularly for solution-phase photodissociation, nonequilibrium effects that are not predicted by LR, such as solvent caging, control the reaction dynamics at intermediate times.[15−18]

The LR approximation assumes that the solvent fluctuations during nonequilibrium dynamics are the same as those present at equilibrium.[1,19,20] There have been numerous studies exploring the success or failure of LR in predicting nonequilibrium reaction dynamics and investigating the conditions where LR can be expected to apply.[3,14,21−32] LR is expected to hold when the solvent fluctuations coupled to the reaction coordinate obey Gaussian statistics and to fail when the fluctuations of just a few molecules deviate from Gaussian behavior.[24,33,34] LR also can fail when the solvent response occurs on a time scale similar to changes in a solute's physical or electronic structure.[18,26,32] Some notable examples of LR breakdown include the rotational coherence of a rigid rotor,[25] solutes that undergo a dipole reversal upon excitation,[14,34,35] solutes that undergo significant changes in size and shape,[27,31,36] and certain electron transfer reactions.[22,23,31] There is also theoretical work arguing that LR can be nonstationary if the equilibrium solvent fluctuations change along a reaction coordinate.[35]

Yet for all the previous studies on solvent dynamics, virtually none have explored how solvent effects change during chemical reactions that explore a wide range of solvent environments. This is the question that serves as the focus of this paper: how does the solvent respond when the solute undergoes a large change in configuration? This is exactly the case for the numerous chemical reactions involving the making and breaking of chemical bonds, including solution-phase photodissociation. As bonds lengthen or are formed, how does the solvent respond, and is the response predictable via LR? To

Received: May 31, 2022
Accepted: July 14, 2022
Published: July 20, 2022

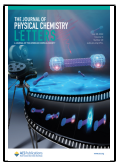

https://doi.org/10.1021/acs.jpclett.2c01656
J. Phys. Chem. Lett. 2022, 13, 6783−6791

answer these questions, we use quantum molecular dynamics simulations to examine how solvent dynamics change through the course of chemical bond breaking, investigate the dramatically different solvent environments an expanding chemical bond can experience, and explore the reasons why the LR approximation fails.

The particular system we focus on is the photodissociation of the Na_2^+ molecule in liquid Ar. We chose Ar as our solvent for several reasons. First, Ar has spherically symmetric interactions with the solute that are dominated by Pauli repulsion; that is, Ar exhibits no favorable bonding motifs such as dative or hydrogen bonds that can alter the chemical identity of the solute, as we have observed previously with Na_2^+ dissolved in liquid THF.[11] Second, as an atomic liquid, Ar provides a particularly simple environment for examining solvent coupling to solute degrees of freedom, as it is apolar and its response can consist only of translational motions. We also chose this system because in previous work we performed simulations of how liquid Ar alters the electronic and vibrational structure of quantum mechanically treated Na_2^+, and we examined how nonequilibrium solvent caging alters the photodissociation dynamics of Na_2^+ relative to that in the gas phase, providing a reference point for this study.[11,18]

In this work, we show that, following photoexcitation of Na_2^+, the solvent dynamics of liquid Ar change discretely at distinct values of the Na_2^+ bond length. In other words, despite the fact that Ar atoms can only translate, the way that Ar translational motions affect the solute's energy gap dramatically changes as the solute moves along its reaction coordinate. We further show that the presence of distinct solvation environments is a quantum mechanical effect where the distinct solvation environments arise from the way solvent molecules interact with the node of the quantum mechanical wave function via Pauli repulsion. This effect is something that could not be captured with a classical description of the excited-state solute. We also find that the solvent dynamics at the earliest times after photoexcitation do not follow either the ground- or excited-state equilibrium dynamics, constituting a failure of LR by any measure, nonstationary or otherwise. Instead, we see that the initial solvent dynamics are driven by just a few solvent atoms whose motions relative to the dissociating Na_2^+ modulate the solute electronic structure in ways that cannot occur at equilibrium.

The computational methods employed in this work are detailed in the Supporting Information. Briefly, we treat the Na_2^+ molecule as two classical Na^+ cores that are held together by a single quantum mechanically treated valence bonding electron. We utilize previously developed pseudopotentials[37] to describe the Na^+-e^- and $Ar-e^-$ interactions.[9,38,39] We solve the Schrödinger equation for the electron in a basis of 32^3 grid points. This methodology reproduces gas-phase quantum chemistry calculations of the Na_2^+ molecule quite well.[11,39] Here, we calculate the behavior of Na_2^+ in liquid Ar, with 1600 solvent atoms, in the canonical (N, V, T) ensemble at 120 K at a density of 1.26 g/mL, well in the liquid region of the phase diagram. In addition to simulations at equilibrium with fixed solute bond lengths on either the ground or electronic excited state, we also ran a nonequilibrium ensemble of 100 trajectories in which uncorrelated equilibrium ground-state configurations were suddenly switched to the excited state to mimic photodissociation. A representative "movie" of a nonequilibrium photodissociation trajectory is given in the Supporting Information.

The standard approach to examining nonequilibrium solvent dynamics is through the calculation of solvation correlation functions. LR theories approximate the nonequilibrium solvent response by using either the equilibrium ground- or excited-state dynamics. The connection between both equilibrium sets of dynamics and nonequilibrium dynamics is well described elsewhere.[33] It is worth noting that although the connection to ground-state dynamics relies on a perturbation from equilibrium, the connection to excited-state dynamics can be made solely by assuming Gaussian statistics.[24,33]

Under LR, the nonequilibrium solvent fluctuations, which are described by a normalized nonequilibrium solvent response function,

$$S(t) = \frac{\langle \Delta E(t) \rangle_{ne} - \langle \Delta E(\infty) \rangle_{ne}}{\langle \Delta E(0) \rangle_{ne} - \langle \Delta E(\infty) \rangle_{ne}} \tag{1}$$

are well approximated by an equilibrium solvation time correlation function, that is,

$$S(t) \approx C_{g/e}(t) = \frac{\langle \delta\Delta E(0)\delta\Delta E(t) \rangle_{g/e}}{\langle (\delta\Delta E(0))^2 \rangle_{g/e}} \tag{2}$$

where $\langle ... \rangle_{ne}$ indicates a nonequilibrium average, $\langle ... \rangle_{g/e}$ indicates an equilibrium ensemble average on the solute ground (g) or excited (e) state, and $\delta\Delta E(t) = \Delta E(t) - \langle \Delta E \rangle$ is the fluctuation of the solute energy gap, ΔE, away from its average value at equilibrium. The connections between $S(t)$ and $C(t)$ have been described in detail elsewhere.[24,28,30,32,35]

For our Na_2^+ solute, the energy gap between the electronic ground and excited states can be altered not only by solvent fluctuations but also from changes in the solute bond length, r. Therefore, to isolate the effects of solvent relaxation on the solute electronic structure, we subtract the gas-phase solute energy gap at each bond distance such that

$$\Delta E_{solv}(r(t)) = E_e(r(t)) - E_g(r(t)) - \Delta E_{gas}(r) \tag{3}$$

We use this definition of the solvent contribution to the solute electronic energy gap for all of the discussion below.

For Na_2^+ in liquid Ar, Figure 1 shows equilibrium solvent time correlation functions, $C(t)$, as a function of the Na^+-Na^+ solute bond length, which is held fixed for this series of simulations, from the Franck–Condon region (3.8 Å) out to the dissociation limit (9.0 Å). Figure 1a shows the bond-distance-dependent equilibrium response when Na_2^+ is on its electronic ground state, $C_g(t)$, while Figure 1b shows that when the solute is held on its lowest electronic excited state, $C_e(t)$. For comparison, the black curve in Figure 1c shows the nonequilibrium solvent response, $S(t)$, following excitation of Na_2^+ from its ground to its dissociative electronic excited state. The figure makes clear that neither the ground- nor the excited-state equilibrium fluctuations at any solute bond distance can accurately predict the nonequilibrium dynamics. Instead, the nonequilibrium solvent relaxation, particularly at early times when the response is expected to consist of the inertial translational motions of the Ar solvent atoms, is faster than the regression of the equilibrium fluctuations on either electronic state.

Of course, one would expect LR to break down in situations where the time scale of solvent rearrangement is comparable to or slower than the time scale of the reaction,[26,32] something that we have previously observed in this system.[18] Moreover, LR also tends to fail when the dynamics are driven by the

https://doi.org/10.1021/acs.jpclett.2c01656
J. Phys. Chem. Lett. 2022, 13, 6783−6791

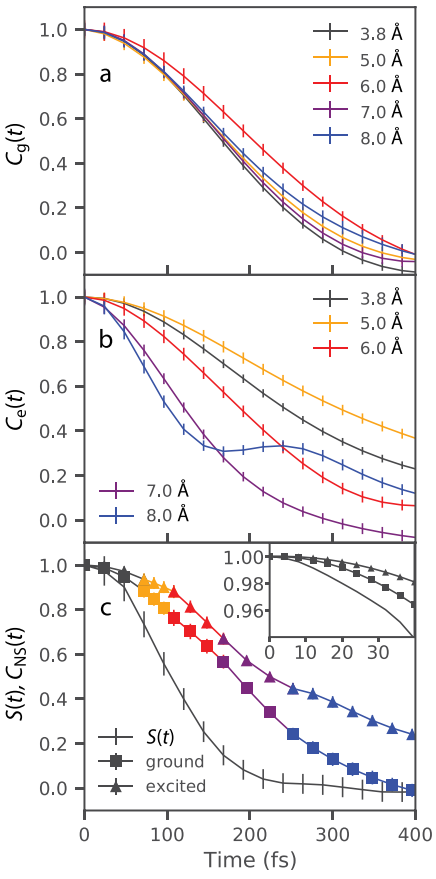

Figure 1. Equilibrium solvation time correlation functions (eq 2) and the nonequilibrium solvent response function (eq 1) following photoexcitation of Na_2^+ in liquid Ar; all the correlation functions use just the solvation component of the energy gap (eq 3). The ground-state equilibrium correlation functions shown in (a) are evaluated at a series of distances along the Na_2^+ bond length reaction coordinate starting from 3.8 Å, the Franck−Condon region, out to 9.0 Å, the dissociation limit of the molecule. The excited-state equilibrium correlation functions evaluated along the bond distance reaction coordinate are shown in (b). (c) Nonequilibrium solvent response function as the solid black curve as well as two nonstationary equilibrium correlation function predictions, $C_{NS}(t)$, one using ground-state fluctuations (squares) and the other using excited-state fluctuations (triangles); the colors show the equilibrium correlation functions that are used to construct the nonstationary prediction (see text for details). Clearly, none of the equilibrium solvent response functions, including the nonstationary ones, can correctly predict the nonequilibrium behavior, even at early times (inset). The error bars presented are for the standard error.

motion of just a few molecules so that the fluctuations are not Gaussian,[25,32,34] as is the case when solutes undergo changes in size or shape.[27,31,36] For our Na_2^+ in a liquid Ar system, the nonequilibrium dissociation dynamics are strongly affected by solvent caging, which is an event that involves only a few solvent molecules,[15,17,18] so it might not appear surprising that standard LR approaches fail. What is surprising, however, is that the solvent motions that cause LR to fail precede caging and that the nature of the solvent fluctuations changes discretely as the solute bond length expands, both at and away from equilibrium, as we discuss further below.

Looking at the solvent response as a function of Na^+−Na^+ bond distance, Figure 1a demonstrates that the equilibrium ground-state energy gap solvent fluctuations are quantitatively similar, no matter what the bond length of the Na_2^+ solute. In contrast, Figure 1b shows that the equilibrium excited-state energy gap solvent fluctuations change significantly as the solute bond is stretched, with the solvent relaxation becoming faster at longer bond distances. This opens the possibility that LR might hold in the Na_2^+/Ar system, but in a nonstationary fashion. The idea of nonstationary LR was proposed by Geissler and Chandler, who studied the solvent dynamics following a solute dipole reversal in liquid water and argued that solvent fluctuations could be Gaussian but not stationary: in other words, the LR-predicted equilibrium solvent dynamics can change at different places along the reaction coordinate. This means that nonequilibrium relaxation might be thought of as proceeding through a series of different equilibrium relaxation dynamics in a nonstationary LR limit.[35]

The colored curves in Figure 1c show two attempts to describe the nonequilibrum relaxation dynamics using a nonstationary LR prediction. The idea is that since the equilibrium solvent response depends on the bond length of the sodium dimer cation (Figure 1a,b), that is, the reaction coordinate of the system, the nonequilibrium response might follow a reaction-coordinate-dependent LR prediction.[35] One way to construct such a nonstationary response function from our simulations would be based on nonstationary Gaussian statistics, expressing the bond-length-dependent decay of the solvation response as $\exp(-kt)$, where $k = k(r)$ and $r = r(t)$. Because the solvation response changes with values of r, a nonstationary solvent response may be constructed as a piecewise addition of the equilibrium solvent response functions; details of how we do this are presented in the Supporting Information. For example, on average, the dimer dissociates to a bond length of 5.0 Å after 72 fs, so the nonstationary correlation function switches from a stationary equilibrium correlation function associated with 3.6 Å to that associated with 5.0 Å after 72 fs. A plot of the nonequilibrium average of $r(t)$, $\langle r(t)\rangle_{ne}$, is included in the Supporting Information for reference. The nonstationary LR prediction using ground-state fluctuations is shown with square markers, and that using excited-state fluctuations is shown with triangular markers; the different colors show the equilibrium correlation "pieces" that contribute to the nonstationary total by using the same color scheme as in panels a and b. What we see is that neither nonstationary correlation function predicts the nonequilibrium relaxation, even at the earliest times prior to caging (Figure 1c, inset) when the solvent response should be largely inertial. Thus, LR breaks down for describing the solvent motions associated with chemical bond breaking, even when nonstationarity is taken into account.

To understand the role that different solvent motions play at and away from equilibrium for the Na_2^+/Ar system, we analyzed the solvent fluctuations that affect the quantum mechanical energy gap of the solute. Figure 2 plots the natural logarithm of the distribution of solvent-induced changes in solute energy gap, creating an effective solvation free energy surface similar to those used in the Marcus theory of electron transfer.[22,40−42] Panel a shows that the way the solvent affects the solute's electronic structure is quite different when the solute is at equilibrium on the electronic ground state (squares), on the electronic excited state (triangles), and during the nonequilibrium dissociation dynamics (vertical lines). None of the three free energy surfaces are parabolic, indicating that the solvent fluctuations that underlie these surfaces are not Gaussian (see the Supporting Information for

https://doi.org/10.1021/acs.jpclett.2c01656
J. Phys. Chem. Lett. 2022, 13, 6783−6791

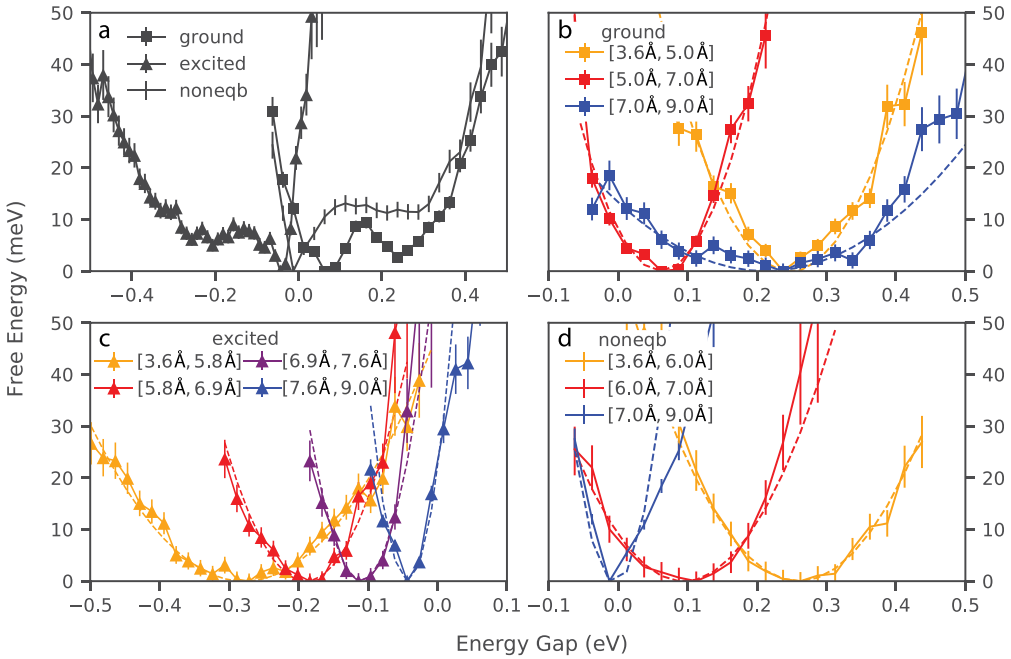

Figure 2. Solvation free energy surfaces, computed as the natural logarithm of the solvation energy gap (eq 3) distributions, for the dissociation of Na_2^+ in liquid Ar. (a) Results along the ground-state equilibrium surface (squares), excited-state equilibrium surface (triangles), and the nonequilibrium surface (vertical lines). These distributions can be well described by either three or four parabolas associated with the solvent fluctuations at different Na_2^+ bond lengths; the way the ground-state free energy surface is composed of solvent fluctuations associated with different solute bond lengths is shown in (b), the excited-state surface in (c), and the nonequilibrium behavior in (d). Clearly, the same translational motions of liquid Ar affect the Na_2^+ solute's energy gap differently as the bond length changes during the photodissociation reaction. The error bars presented are for the standard error.

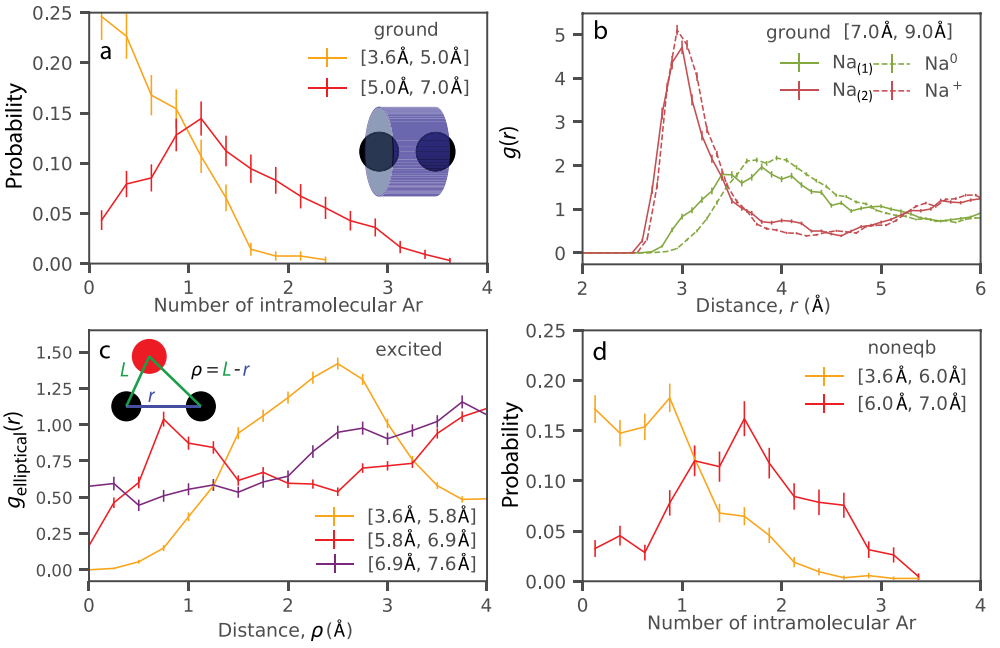

Figure 3. Structural changes in the local solvent environment as the Na_2^+ dimer in liquid Ar dissociates along different pathways. (a, b) Changes in structure at equilibrium on the ground state for different Na_2^+ bond lengths, with (a) showing the number of Ar atoms in a cylinder around the intramolecular region, as depicted in the inset. Ar atoms within this region more strongly affect the energy gap due to high density of the ground-state wave function and sparse density of the excited-state wave function. (b) Na^+−Ar radial distribution functions, where $Na_{(1)}$ is the Na^+ core closest to the bonding electron's center of mass and $Na_{(2)}$ is the other Na^+ core; at long solute bond lengths, the electron localizes on $Na_{(1)}$ to form Na^0 and Na^+ dissociation products. (c) Solvation structure at equilibrium on the excited state using an elliptical distribution function defined according to the schematic in the inset and discussed in the main text. For small excited-state Na_2^+ bond lengths (≤5.8 Å), Ar atoms can only come within ρ = 2 Å of the intramolecular region. As the bond length increases, Ar atoms can move to reside between the Na^+ cations on the bond axis, shown by the increase at ρ = 0 Å for Na^+−Na^+ distances ≥6.9 Å. (d) Intramolecular Ar distribution, the same as in (a), for different bond length ranges during the nonequilibrium dissociation dynamics. The error bars presented are for the standard error.

https://doi.org/10.1021/acs.jpclett.2c01656
J. Phys. Chem. Lett. 2022, 13, 6783−6791

details), which is one of the hallmarks of LR breakdown.[24,25,32−34]

All three of the solvation free energy surfaces in Figure 2a, however, fit well to the sum of just a few parabolas that arise at different Na_2^+ bond lengths. For example, Figure 2b shows that the ground-state solvation free energy surface is well described as the sum of three parabolic surfaces: one for solute bond distances between 3.6 and 5.0 Å (yellow squares), one for distances between 5.0 and 7.0 Å (red squares), and one for nearly dissociated Na_2^+ with bond distances greater than 7.0 Å (blue squares). In a similar fashion, Figure 2c shows that the excited-state solvation free energy surface is composed of four parabolas, separated by bond lengths at 5.8, 6.9, and 7.6 Å, while Figure 2d indicates that the nonequilibrium dynamics following photoexcitation are well-described by three parabolas separated by bond lengths at 6.0 and 7.0 Å.

The fact that these solvation free energy surfaces fit to parabolas with different curvatures at distinct Na_2^+ bond lengths suggests that the solute encounters unique solvent environments as it dissociates. In other words, the solvent motions that modulate the solute energy gap fluctuate in one particular way when the bond length is small and suddenly fluctuate in a different way as the bond extends. The way the fluctuations change with bond length is different for the equilibrium ground state as well as the equilibrium excited state and during the nonequilibrium dynamics. This is remarkable because the liquid Ar solvent in this system can undergo only translational motions, meaning that the same solvent motions affect the solute's quantum energy gap differently as the bond length changes. Thus, rather than experiencing a continuous change of solvent environments, the dissociating solute encounters a small handful of discrete, distinct environments. As described further below, the presence of these distinct environments explains the solute bond-length-dependent correlation functions seen in Figure 1 and provides a rationale for the way LR breaks down in this system.

Given that the Ar interaction with Na_2^+ is isotropic and that Ar can only translate, why are there discrete solvation signatures both at and away from equilibrium? We begin answering this question by examining dissociation along the ground-state equilibrium pathway. Near the equilibrium bonding distance, the Na_2^+ electronic ground-state wave function is roughly a σ molecular orbital with a prolate spheroidal shape (see, e.g., Figure 1b of ref 10 as well as the Supporting Information). On the other hand, the excited-state wave function, roughly a σ^* antibonding molecular orbital, has a node between the two Na^+ cores. As the Na_2^+ molecule's bond lengthens, there comes a point near 5 Å when the Na_2^+ bond length is large enough that an Ar atom can fit between the two Na^+ cores, as demonstrated further below in Figure 3a. The presence of this solvent atom in the intramolecular region modulates the solute energy gap differently from other surrounding Ar atoms because of the node in the excited-state wave function. Finally, at even longer bond lengths, starting around 7 Å, the solvent breaks the local molecular symmetry, causing the bonding electron to localize onto one of the two sodium cations: once dissociated, the electronic structure becomes that of a neutral Na atom plus sodium cation rather than a molecular dimer cation; this localization is evident in the representative nonequilibrium trajectory movie shown in the Supporting Information.

To visualize the changes in solvent structure when the Na_2^+ bond length reaches 5 Å, Figure 3a shows the average number of Ar atoms in the intramolecular region. The calculation is performed by integrating over a cylinder centered on the dimer, where the length of the cylinder is equal to the solute bond length and the radius of the cylinder is 3.0 Å, which is the average first-shell Na^+−Ar distance, as shown in Figure 3b. As the Na_2^+ bond length increases beyond 5 Å, the most probable number of Ar atoms in the intramolecular region increases from zero to one. The Ar atom located in the intramolecular region has a stronger interaction with the ground-state wave function than other Ar atoms but less overlap with the excited-state wave function than other Ar atoms because of the excited-state node, as shown explicitly in the Supporting Information. Thus, the second solvation free energy parabola in Figure 2b, for bond lengths between 5.0 and 7.0 Å, results from the introduction of intramolecular Ar atoms that destabilize the ground-state energy while moderately stabilizing the excited-state energy. The fluctuations of these intramolecular Ar atoms more strongly affect the solute's energy gap than the motions of other Ar atoms, resulting in a steeper parabolic free energy surface.

To characterize the solvent structure for the third solvation regime at long Na_2^+ bond distances in Figure 2b, for bond lengths between 7.0 and 9.0 Å, we calculated the radial distribution function of the Ar solvent atoms around each Na^+ core (solid curves in Figure 3b). In this figure, we differentiate the two Na^+ cores by labeling $Na_{(1)}$ as that which is closer to the bonding electron's center of mass and $Na_{(2)}$ as that which is further away. Defined this way, we see that $Na_{(1)}$ (green solid curve) has its first Ar solvation shell at 3.8 Å, with a peak height of ∼2, while $Na_{(2)}$ (red solid curve) shows its first solvation shell peak at 3.0 Å, with a peak height of nearly 5. The two different pair distribution functions match well with those of isolated neutral sodium atoms and sodium cations in liquid Ar, respectively (dashed curves). Thus, the distinct solvation regime in Figure 2b at long Na^+−Na^+ distances is due to the bonding electron being localized by the solvent to produce Na^0 and Na^+ dissociation products, a quantum mechanical phenomenon. Ar solvent motions affect the neutral atomic Na^0 energy gap differently than the ionic Na_2^+ cation gap, explaining the different curvature of the solvation free energy parabola for these bond distances in Figure 2b.

To characterize the solvent structures along the excited-state equilibrium pathway, we found it best to use an elliptical distribution function, which is shown in Figure 3c. Like a radial distribution function, the elliptical distribution function we show in Figure 3c counts Ar atoms within a defined region of space around the dimer, but instead of radial distances, it counts according to an elliptical criterion, L, which is the sum of the distances between an Ar atom and each Na^+ core. Plotted on the horizontal axis of Figure 3c is the difference between the elliptical criterion, L, and the Na^+−Na^+ distance, r, to create a common axis, $\rho = L - r$, for ease of comparison. Defined this way, a value of $\rho = 0$ Å would identify Ar atoms positioned directly along the bond axis, while a value of $\rho = 2$ Å would identify first-shell Ar atoms in the Na_2^+ intramolecular region that lie ≈2 Å away from the bond axis, as illustrated in the schematic shown in the inset. As Na_2^+ dissociates, the solvent rearranges so that first-shell Ar atoms that were outside the bond axis can now lie along the bond axis, which can be seen in the rise in the elliptical distribution at $\rho = 0$ Å and the fall between $\rho = 1$ Å and $\rho = 3$ Å. Like the change in solvent

https://doi.org/10.1021/acs.jpclett.2c01656
J. Phys. Chem. Lett. 2022, 13, 6783−6791

structure seen at 5.0 Å for the ground-state equilibrium dissociation (Figure 3a), this change in packing leads to a greater interaction of intramolecular Ar atoms with the ground-state wave function than the excited-state wave function of the solute and thus a distinct solvent fluctuation signature with a steeper parabola as the dimer dissociates and Ar atoms can reach the bond axis between the Na nuclei.

The change in solvent environment along the excited-state equilibrium pathway at Na_2^+ bond lengths greater than 7.6 Å can be understood by the fact that the ground and excited states of the solute are becoming degenerate. (For reference, the ground- and excited-state energies with the solvent held in equilibrium with the excited-state solute are shown in ref 18.) Because the electronic states are quasi-degenerate at the dissociation limit, the energy gap is necessarily close to 0 eV with small fluctuations, as observed in Figure 2c. It is worth noting that in the dissociation limit the ground- and excited-state wave functions have the electron on different Na^+ cores (the roles of Na^0 and Na^+ are reversed on the electronic ground and excited states), so that when the two states are degenerate, they are also equally solvated. In the Supporting Information, we calculate the Ar−electron overlap for each solute energy state in the 7.6−9.0 Å bond length range and show that the overlap of Ar atoms with the excited state is indeed identical with that of the ground state.

Although our finding that there are discrete solvation environments along the equilibrium dissociation pathways was unexpected, the main motivation of this work is to understand the nature of the nonequilibrium solvation dynamics during photodissociation, shown in Figure 2d. Away from equilibrium, the dimer cation encounters three distinct solvent environments, at solute bond lengths less than 6 Å, between 6 and 7 Å, and for bond separations greater than 7 Å. The initial nonequilibrium solvation free energy distribution (yellow curve in Figure 2d) is clearly more similar to that of the ground-state distribution (yellow squares in Figure 2b), while the nonequilibrium solvation free energy surface at later times (blue curve in Figure 2d) is more similar to that of the excited state (blue triangles in Figure 2c). This change in behavior from more ground-state-like to more excited-state-like is in line with expectations,[12−14] but the nonequilibrium solvent fluctuations still do not match any of the equilibrium distributions.

Of course, one feature that affects the nonequilibrium dynamics of dissociating Na_2^+ in liquid Ar that is not present at equilibrium is solvent caging, which we have previously investigated for this system.[18] On average, the dimer cation dissociates to a Na^+−Na^+ distance of 6.0 Å after 100 fs, which is the average time when the Na^+ cores collide with their first-shell Ar solvent atom neighbors. Along with this caging event, we also observe an increase in the number of intramolecular Ar atoms (Figure 3d) at this distance, similar to what we described above for the ground-state equilibrium at 5.0 Å separation; the intramolecular Ar atoms do not appear until larger bond distances in the nonequilibrium dynamics because given the inertia of the solvent atoms, there simply is not time for Ar to "notice" the empty space between the separating Na atoms. Once the Na_2^+ bond length reaches 7.0 Å, the solvation dynamics are determined by the near-degeneracy of the ground and excited states, much like what we described above for the excited-state equilibrium, where the fluctuating energy gap is necessarily centered at zero with minimal spread.

With this understanding of how the nonequilibrium solvent environment changes with solute bond distance, we return to discuss the origins of the breakdown of LR seen at early times seen in Figure 1c. Although solvent caging, the strong collision of the dissociating solute with the first-shell solvent atoms, is a single-solvent-atom effect that is expected to lead to a breakdown of LR,[15,17,18] caging does not take place until ≥100 fs after photoexcitation. Instead, the more rapid relaxation of the nonequilibrium energy gap at early times that is the hallmark of LR breakdown can be explained by the motion of the dissociating Na^+ cations creating relative Ar motions that help to rapidly close the energy gap. In other words, the breakdown of LR is entirely a quantum mechanical effect that directly involves the electronic structure of the Na_2^+ solute on its ground and electronic excited states; this breakdown would not have been observed had we described the system on a potential of mean force using classical molecular dynamics.

To understand how relative solute−solvent motions affect the dissociating solute's quantum energy gap, we performed gas-phase calculations of a dissociating Na_2^+ dimer interacting with a single Ar solvent atom; details of how we performed these calculations are included in the Supporting Information. The idea is that when Na_2^+ is promoted to its dissociative excited state, the rapidly expanding solute effectively moves Ar atoms toward the solute center of mass. Ar atoms that lie along the expanding solute bond axis move toward the Na^+ cores (Figure 4a), while Ar atoms that are displaced from the bond axis move parallel to the bond toward the intramolecular region (Figure 4b). Because Ar atoms undergo relative motion toward the solute, the distances shown in Figures 4a and 4b are plotted with larger Ar−Na distances to the left, so that time following the photodissociation proceeds from left to right. The distance ranges shown approximately reflect the relative Ar motions over the first 100 fs following photoexcitation, prior and up to the caging event.

Figure 4a shows that relative motion of axial Ar atoms moving toward the expanding Na_2^+ solute causes a large change in the quantum energy gap. The excited-state wave function has a larger axial extent than the ground-state wave function, so Pauli repulsion interactions from the approaching solvent atom raise the solute's excited-state energy. In contrast, the same axial motion of solvent atoms toward the solute leads to slight stabilization of the ground-state energy due to van der Waals forces. Figure 4b shows that for Ar atoms that are displaced from the bond axis the effect of relative solvent motion toward the solute is opposite, stabilizing the excited state and destabilizing the ground state. Because of the node in the excited-state wave function, the presence of Ar in the intramolecular region leads to van der Waals stabilization, while the nodeless ground-state wave function experiences strong Pauli repulsion from the overlapping Ar atom in this region. During the nonequilibrium dissociation dynamics, both types of relative solvent motion—along the bond axis and "above" the bond axis into the intramolecular region—occur. In combination, these motions lead to net destabilization of the ground state and relatively little change in the excited-state energy (see the Supporting Information for more details). This quantum mechanical effect is what causes the nonequilibrium energy gap to close more quickly than at equilibrium on either the ground or the excited state, leading to the breakdown of LR seen in Figure 1c. This mechanistic picture of how LR breaks down is reminiscent of other systems where LR fails

https://doi.org/10.1021/acs.jpclett.2c01656
J. Phys. Chem. Lett. 2022, 13, 6783−6791

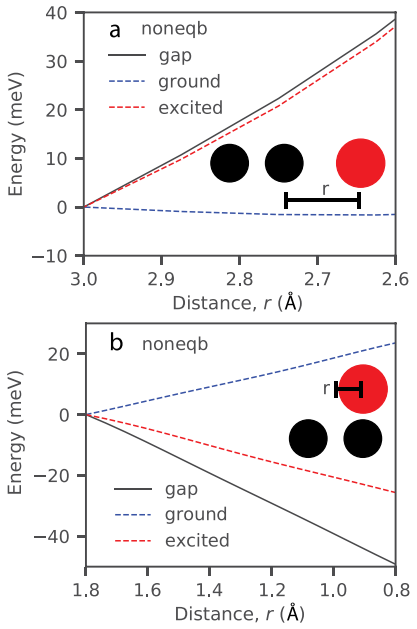

Figure 4. (a) Effect on the Na_2^+ energy gap (black curve) of a single non-intramolecular Ar atom moving along the sodium dimer cation bond axis toward one of the Na^+ cores: because the excited-state Na_2^+ molecular orbital extends further along the bond axis, Ar motions along the bond axis destabilize the excited-state energy (red dotted curve) more than the ground-state energy (blue dashed curve). (b) Effect on the Na_2^+ energy gap (black curve) of a single Ar atom that sits 3.0 Å above the bond axis moving parallel to the bond axis toward the intramolecular region: because of the presence of the node in the excited-state molecular orbital, Ar motion along this axis tends to stabilize the excited-state energy (red dashed curve) and destabilize the ground state (blue dashed curve). The distance axis is defined separately for each panel, and each panel includes a cartoon to illustrate the motion being considered. The distance axis is plotted with larger distances to the left so that reading from left to right follows the relative Ar motion with time following photoexcitation: 100 fs after excitation, axial Ar atoms are ~2.6 Å away from the Na^+ cores, and Ar atoms that are displaced from the bond axis have moved to reside 1.0 Å from the intramolecular region. These differences explain why the solute encounters distinct solvent environments as it dissociates.

because of the motions of just a few solvent molecules.[25,27,31,32,34,36]

In summary, through MQC MD simulations of the photodissociation of Na_2^+ in liquid Ar, we have explored how solvent fluctuations change during the course of a bond breaking reaction. In the process, we tested both standard approaches and a nonstationary approach to LR and find that neither LR approach captures the nonequilibrium solvent fluctuations at early times (Figure 1). We find that the energy gap distributions can be fit to a few Gaussians that are well separated by solute bond length and have unique curvatures, indicating discrete changes in solvent environment (Figure 2). If the dimer dissociates along the ground-state equilibrium surface, it will encounter three distinct solvent environments, with one new environment induced by an increase in the number of intramolecular Ar atoms (Figure 3a) and a second induced by localization of the electron to form $Na^+ + Na^0$ (Figure 3b). If the dimer dissociates along the excited-state equilibrium surface, then it will encounter four distinct solvent environments, with the one at the longest bond distances caused by the near solvation energy degeneracy of the two Na^+ cores on the ground and electronic excited states. The intermediate excited-state environments result from changes in solvation structure that are best captured by using an elliptical distribution function (Figure 3c). When nonequilibrium dissociation is initiated by photoexcitation, the solute encounters three distinct solvent environments including the Franck−Condon region. One change in environment results from solvent caging and the driven collision of the photofragments with the first solvent shell, and the second new environment at long bond lengths arises from degeneracy as with the equilibrium excited state. Although the initial nonequilibrium solvent environment in the Franck−Condon region is structurally identical with that of the equilibrium ground state, the solvation dynamics away from equilibrium are significantly different because of dissociation-driven relative Ar motions that quickly close the energy gap (Figure 4a,b). The effect of these nonequilibrium relative motions on the solute energy gap is entirely quantum mechanical in nature, and these motions also explain the early time (precaging) breakdown of LR for this system.

Overall, even for an isotropic, repulsive, apolar solvent that can undergo only translational motions, such as liquid Ar, solvent environments and the way their fluctuations couple to the electronic structure of solutes can change suddenly and dramatically during the course of bond breaking or bond formation. We close by noting that the changes in solvent response result from changes in solute geometry that change the quantum mechanical interactions between the solute and solvent. Because of the fact that solutes encounter distinct solvent environments as their bond length changes, the solvent response depends on the reaction pathway taken, highlighting the complexity of solution-phase solvation dynamics. We expect that these observations should be generally applicable for solution-phase chemistry, including bond breaking, bond formation, ion pairing and unpairing, and electron transfer reactions where there are significant changes in geometry of the donor and acceptor or when the reaction proceeds through a solvent-separated structure.[43−45]

■ ASSOCIATED CONTENT

Supporting Information

The Supporting Information is available free of charge at https://pubs.acs.org/doi/10.1021/acs.jpclett.2c01656.

Additional details of the simulations and findings as well as a separate movie file showing the dynamics during a representative nonequilibrium dissociation trajectory (PDF)

■ AUTHOR INFORMATION

Corresponding Author

Benjamin J. Schwartz − *Department of Chemistry & Biochemistry, University of California, Los Angeles, Los Angeles, California 90095-1569, United States;* orcid.org/0000-0003-3257-9152; Phone: (310) 206-4113; Email: schwartz@chem.ucla.edu

Author

Andy Vong − *Department of Chemistry & Biochemistry, University of California, Los Angeles, Los Angeles, California 90095-1569, United States*

Complete contact information is available at: https://pubs.acs.org/10.1021/acs.jpclett.2c01656

https://doi.org/10.1021/acs.jpclett.2c01656
J. Phys. Chem. Lett. 2022, 13, 6783−6791

Notes

The authors declare no competing financial interest.

Any data generated and analyzed for this study that are not included in this article and its Supporting Information are available from the authors upon reasonable request.

■ ACKNOWLEDGMENTS

This work was supported by the U.S. Department of Energy Condensed Phase and Interfacial Molecular Science program under Grant DE-SC0017800. We gratefully acknowledge the Institute for Digital Research and Education (IDRE) at UCLA for use of the hoffman2 computing cluster. In addition, this work used the Extreme Science and Engineering Discovery Environment (XSEDE), which is supported by National Science Foundation Grant ACI-1548562.[46]

■ REFERENCES

(1) Voth, G. A.; Hochstrasser, R. M. Transition State Dynamics and Relaxation Processes in Solutions: A Frontier of Physical Chemistry. *J. Phys. Chem.* **1996**, *100*, 13034−13049.

(2) Keaveney, S. T.; White, B. P.; Haines, R. S.; Harper, J. B. The Effects of Ionic Liquid on Unimolecular Substitution Processes: The Importance of the Extent of Transition State Solvation. *Org. Biomol. Chem.* **2016**, *14*, 2572−2580.

(3) Voth, G. A. Computer Simulation of Proton Solvation and Transport in Aqueous and Biomolecular Systems. *Acc. Chem. Res.* **2006**, *39*, 143−150.

(4) Goyal, P.; Schwerdtfeger, C. A.; Soudackov, A. V.; Hammes-Schiffer, S. Proton Quantization and Vibrational Relaxation in Nonadiabatic Dynamics of Photoinduced Proton-Coupled Electron Transfer in a Solvated Phenol-Amine Complex. *J. Phys. Chem. B* **2016**, *120*, 2407−2417.

(5) Sheps, L.; Miller, E. M.; Horvath, S.; Thompson, M. A.; Parson, R.; McCoy, A. B.; Lineberger, W. C. Solvent-Mediated Electron Hopping: Long-Range Charge Transfer in $IBr^-(CO_2)$ Photodissociation. *Science* **2010**, *328*, 220−224.

(6) Margulis, C. J.; Coker, D. F.; Lynden-Bell, R. M. Symmetry Breaking of the Triiodide Ion in Acetonitrile Solution. *Chem. Phys. Lett.* **2001**, *341*, 557−560.

(7) Zhang, F. S.; Lynden-Bell, R. M. Solvent-Induced Symmetry Breaking. *Phys. Rev. Lett.* **2003**, *90*, 185505.

(8) Zhang, F. S.; Lynden-Bell, R. M. Solvent-Induced Symmetry Breaking: Varying Solvent Strength. *Phys. Rev. E* **2005**, *71*, 021502.

(9) Glover, W. J.; Larsen, R. E.; Schwartz, B. J. How Does a Solvent Affect Chemical Bonds? Mixed Quantum/Classical Simulations with a Full CI Treatment of the Bonding Electrons. *J. Phys. Chem. Lett.* **2010**, *1*, 165−169.

(10) Widmer, D. R.; Schwartz, B. J. Solvents Can Control Solute Molecular Identity. *Nat. Chem.* **2018**, *10*, 910−916.

(11) Widmer, D. R.; Schwartz, B. J. The Role of the Solvent in the Condensed-Phase Dynamics and Identity of Chemical Bonds: The Case of the Sodium Dimer Cation in THF. *J. Phys. Chem. B* **2020**, *124*, 6603−6616.

(12) Maroncelli, M. Computer Simulations of Solvation Dynamics in Acetonitrile. *J. Chem. Phys.* **1991**, *94*, 2084−2103.

(13) Kumar, P. V.; Maroncelli, M. Polar Solvation Dynamics of Polyatomic Solutes: Simulation Studies in Acetonitrile and Methanol. *J. Chem. Phys.* **1995**, *103*, 3038−3060.

(14) Ladanyi, B. M.; Maroncelli, M. Mechanisms of Solvation Dynamics of Polyatomic Solutes in Polar and Nondipolar Solvents: A Simulation Study. *J. Chem. Phys.* **1998**, *109*, 3204−3221.

(15) Wang, W. N.; Nelson, K. A.; Xiao, L.; Coker, D. F. Molecular-Dynamics Simulation Studies of Solvent Cage Effects on Photodissociation in Condensed Phases. *J. Chem. Phys.* **1994**, *101*, 9663−9671.

(16) Douady, J.; Jacquet, E.; Giglio, E.; Zanuttini, D.; Gervais, B. Non-Adiabatic Molecular Dynamics of Excited Na_2^+ Solvated in Ar_{17} Clusters. *Chem. Phys. Lett.* **2009**, *476*, 163−167.

(17) Zanuttini, D.; Douady, J.; Jacquet, E.; Giglio, E.; Gervais, B. Nonadiabatic Molecular Dynamics of Photoexcited Li_2^+ Ne_n Clusters. *J. Chem. Phys.* **2011**, *134*, 044308.

(18) Vong, A.; Widmer, D. R.; Schwartz, B. J. Nonequilibrium Solvent Effects During Photodissociation in Liquids: Dynamical Energy Surfaces, Caging, and Chemical Identity. *J. Phys. Chem. Lett.* **2020**, *11*, 9230−9238.

(19) Chandler, D. *Introduction to Modern Statistical Mechanics*; Oxford University Press: New York, 1987.

(20) Truhlar, D. G.; Garrett, B. C.; Klippenstein, S. J. Current Status of Transition-State Theory. *J. Phys. Chem.* **1996**, *100*, 12771−12800.

(21) Stratt, R. M.; Maroncelli, M. Nonreactive Dynamics in Solution: The Emerging Molecular View of Solvation Dynamics and Vibrational Relaxation. *J. Phys. Chem.* **1996**, *100*, 12981−12996.

(22) King, G.; Warshel, A. Investigation of the Free Energy Functions for Electron Transfer Reactions. *J. Chem. Phys.* **1990**, *93*, 8682−8692.

(23) Hammes-Schiffer, S. Theoretical Perspectives on Proton-Coupled Electron Transfer Reactions. *Acc. Chem. Res.* **2001**, *34*, 273−281.

(24) Laird, B. B.; Thompson, W. H. On the Connection Between Gaussian Statistics and Excited-State Linear Response for Time-Dependent Fluorescence. *J. Chem. Phys.* **2007**, *126*, 211104.

(25) Moskun, A. C.; Jailaubekov, A. E.; Bradforth, S. E.; Tao, G.; Stratt, R. M. Rotational Coherence and a Sudden Breakdown in Linear Response Seen in Room-Temperature Liquids. *Science* **2006**, *311*, 1907−1911.

(26) Fonseca, T.; Ladanyi, B. M. Breakdown of Linear Response for Solvation Dynamics in Methanol. *J. Phys. Chem.* **1991**, *95*, 2116−2119.

(27) Aherne, D.; Tran, V.; Schwartz, B. J. Non-Linear, Non-Polar Solvation Dynamics in Water: The Roles of Electrostriction and Solvent Translation in the Breakdown of Linear Response. *J. Phys. Chem. B* **2000**, *104*, 5382−5394.

(28) Bedard-Hearn, M. J.; Larsen, R. E.; Schwartz, B. J. Hidden Breakdown of Linear Response: Projections of Molecular Motions in Nonequilibrium Simulations of Solvation Dynamics. *J. Phys. Chem. A* **2003**, *107*, 4773−4777.

(29) Heid, E.; Moser, W.; Schröder, C. On the Validity of Linear Response Approximations Regarding the Solvation Dynamics of Polyatomic Solutes. *Phys. Chem. Chem. Phys.* **2017**, *19*, 10940−10950.

(30) Heid, E.; Schröder, C. Solvation Dynamics in Polar Solvents and Imidazolium Ionic Liquids: Failure of Linear Response Approximations. *Phys. Chem. Chem. Phys.* **2018**, *20*, 5246−5255.

(31) Bragg, A. E.; Cavanagh, M. C.; Schwartz, B. J. Linear Response Breakdown in Solvation Dynamics Induced by Atomic Electron-Transfer Reactions. *Science* **2008**, *321*, 1817−1822.

(32) Tao, G.; Stratt, R. M. The Molecular Origins of Nonlinear Response in Solute Energy Relaxation: The Example of High-Energy Rotational Relaxation. *J. Chem. Phys.* **2006**, *125*, 114501.

(33) Laird, B. B.; Thompson, W. H. Time-Dependent Fluorescence in Nanoconfined Solvents: Linear-Response Approximations and Gaussian Statistics. *J. Chem. Phys.* **2011**, *135*, 1−13.

(34) Schile, A. J.; Thompson, W. H. Tests for, Origins of, and Corrections to Non-Gaussian Statistics: The Dipole-Flip Model. *J. Chem. Phys.* **2017**, *146*, 154109−154109.

(35) Geissler, P. L.; Chandler, D. Importance Sampling and Theory of Nonequilibrium Solvation Dynamics in Water. *J. Chem. Phys.* **2000**, *113*, 9759−9765.

(36) Bragg, A. E.; Glover, W. J.; Schwartz, B. J. Watching the Solvation of Atoms in Liquids One Molecule at a Time. *Phys. Rev. Lett.* **2010**, *104*, 1−4.

(37) Szaz, L. *Pseudopotential Theory of Atoms and Molecules*; Wiley: New York, 1985.

(38) Gervais, B.; Giglio, E.; Jacquet, E.; Ipatov, I.; Reinhard, P. G.; Suraud, E. Simple DFT Model of Clusters Embedded in Rare Gas

https://doi.org/10.1021/acs.jpclett.2c01656
J. Phys. Chem. Lett. 2022, 13, 6783−6791

Matrix: Trapping Sites and Spectroscopic Properties of Na Embedded in Ar. *J. Chem. Phys.* **2004**, *121*, 8466−8480.
(39) Glover, W. J.; Larsen, R. E.; Schwartz, B. J. The Roles of Electronic Exchange and Correlation in Charge-Transfer-to-Solvent Dynamics: Many-Electron Non-Adiabatic Mixed Quantum/Classical Simulations of Photoexcited Sodium Anions in the Condensed Phase. *J. Chem. Phys.* **2008**, *129*, 164505.
(40) Tachiya, M. Relation Between the Electron-Transfer Rate and the Free Energy Change of Reaction. *J. Phys. Chem.* **1989**, *93*, 7050−7052.
(41) Wu, Q.; Van Voorhis, T. Direct Calculation of Electron Transfer Parameters Through Constrained Density Functional Theory. *J. Phys. Chem. A* **2006**, *110*, 9212−9218.
(42) Zhu, J.; Spirina, O. B.; Cukier, R. I. Solvent Dynamical Effects on Bond-Breaking Electron Transfer Reactions. *J. Chem. Phys.* **1994**, *100*, 8109−8124.
(43) Grabowski, Z. R.; Rotkiewicz, K.; Rettig, W. Structural Changes Accompanying Intramolecular Electron Transfer: Focus on Twisted Intramolecular Charge-Transfer States and Structures. *Chem. Rev.* **2003**, *103*, 3899−4032.
(44) Ghosh, S.; Soudackov, A. V.; Hammes-Schiffer, S. Electrochemical Electron Transfer and Proton-Coupled Electron Transfer: Effects of Double Layer and Ionic Environment on Solvent Reorganization Energies. *J. Chem. Theory Comput.* **2016**, *12*, 2917−2925.
(45) Warburton, R. E.; Soudackov, A. V.; Hammes-Schiffer, S. Theoretical Modeling of Electrochemical Proton-Coupled Electron Transfer. *Chem. Rev.* **2022**, *122*, 10599.
(46) Towns, J.; Cockerill, T.; Dahan, M.; Foster, I.; Gaither, K.; Grimshaw, A.; Hazlewood, V.; Lathrop, S.; Lifka, D.; Peterson, G. D.; et al. XSEDE: Accelerating Scientific Discovery. *Comput. Sci. Eng.* **2014**, *16*, 62−74.

https://doi.org/10.1021/acs.jpclett.2c01656
J. Phys. Chem. Lett. 2022, 13, 6783−6791